

On the Implementation of the Coexistence Phase of Antiferromagnetism and Superconductivity in Heavy-Fermion Intermetallides

V. V. Val'kov^{a, b, *} and A. O. Zlotnikov^a

^a Kirensky Institute of Physics, Siberian Branch, Russian Academy of Sciences, Krasnoyarsk, Russia

^b Siberian State Aerospace University, Krasnoyarsk, Russia

* e-mail: vvv@iph.krasn.ru

Received December 19, 2011; in final form, February 20, 2012

The region of the state diagram in which the pressure-induced quantum phase transition occurs with the destruction of the antiferromagnetic ordering and the appearance of the superconductivity has been described within the periodic Anderson model. It has been shown that a microscopically homogeneous coexistence phase of antiferromagnetism and superconductivity is implemented in the vicinity of the critical point, which was experimentally found in the heavy-fermion compound CeRhIn₅. In this region, the pressure increase is accompanied by the experimentally observed strong growth of the effective fermion mass.

DOI: 10.1134/S0021364012070089

1. A coexistence phase of antiferromagnetism and superconductivity was recently observed in a series of heavy-fermion compounds (see, e.g., review [1]). In Ce-based heavy-fermion compounds, the coexistence phase of antiferromagnetism and superconductivity is often achieved by the change in the ground state due to the application of an external hydrostatic pressure. For example, CeIn₃ [2], CeRhIn₅ [3], and Ce₂RhIn₈ [4] are considered as such compounds.

A phenomenological two-liquid model was proposed in [5] on the basis of experimental data. This model made it possible to describe the thermodynamic, magnetic, and transport properties of many heavy-fermion materials. Its main idea is connected with the existence of the coherence temperature T^* below which the thermodynamic characteristics are determined by two different contributions. The first contribution is due to the presence of Kondo impurities. The second contribution is determined by the hybridization processes of localized electrons with the conduction electrons leading to the formation of the heavy-fermion coherent state. The temperature T^* is related to the parameter $\epsilon = J_{sd}\rho(E_F)$, where J_{sd} is the integral of the s – d exchange interaction and $\rho(E_F)$ is the density of states on the Fermi level. For a series of heavy-fermion compounds, the parameter ϵ is directly related to the type of phase transition at low temperatures [6]. In [7], a mechanism was proposed according to which the transition from the antiferromagnetic phase to the superconducting phase with increasing external pressure is explained by the growth of ϵ .

In the phenomenological approach, the problem of the microscopic mechanisms determining the struc-

ture of the phase diagram of, e.g., CeRhIn₅, remains open. Furthermore, an important question of whether different interactions or the same interaction induces transitions to the superconducting and antiferromagnetic states is not considered. The possibility of implementing the coexistence phase of antiferromagnetism and superconductivity in heavy-fermion systems was considered on the microscopic level in [8, 9].

In this work, we show that the microscopic mechanism of forming the coexistence phase of antiferromagnetism and superconductivity with the d -wave superconducting order parameter can be related to the presence of the exchange interaction in the subsystem of the localized moments. The calculations were performed on the basis of the effective periodic Anderson model, which takes into account the superexchange interaction in a system of localized f electrons. The conditions under which the coexistence phase of antiferromagnetism and superconductivity corresponding to that observed experimentally is implemented were obtained. The proposed model reflects well the features of the electron structure of Ce-based heavy-fermion intermetallides (e.g., CeRhIn₅), since the same Ce $4f$ electrons in them are responsible for the establishment of the antiferromagnetic ordering and superconductivity [10]. An important conclusion obtained in [11] is that two-liquid behavior is possible for this model. The mentioned exchange interaction arises when the high-energy processes are taken into account [12]. The appearance temperatures of the antiferromagnetic phase and superconductivity in heavy-fermion systems are several times less than T^* . In this region, the behavior of the system is mainly

determined by heavy fermions (up to 90% [5]) rather than by the isolated Kondo impurities.

2. We write the effective Hamiltonian of the periodic Anderson model in the strong correlation regime in the form

$$\hat{\mathcal{H}}_{\text{eff}} = \hat{\mathcal{H}}_{c0} + \hat{\mathcal{H}}_{f0} + \hat{\mathcal{H}}_{\text{mix}} + \hat{\mathcal{H}}_{\text{exch}},$$

where

$$\begin{aligned} \hat{\mathcal{H}}_{c0} &= \sum_{m\sigma} (\varepsilon_0 - \mu) c_{m\sigma}^\dagger c_{m\sigma} + \sum_{ml\sigma} t_{ml} c_{m\sigma}^\dagger c_{l\sigma}, \\ \hat{\mathcal{H}}_{f0} &= \sum_{m\sigma} (E_0 - \mu) X_m^{\sigma\sigma}, \\ \hat{\mathcal{H}}_{\text{mix}} &= \sum_{ml\sigma} (V_{ml} c_{m\sigma}^\dagger X_l^{0\sigma} + \text{H.c.}), \\ \hat{\mathcal{H}}_{\text{exch}} &= \frac{1}{2} \sum_{ml} J_{ml} \left(\mathbf{S}_m \mathbf{S}_l - \frac{1}{4} \hat{N}_m \hat{N}_l \right). \end{aligned} \quad (1)$$

Subscripts m and l denote the m th and l th sites of the lattice in the Wannier representation, respectively. The calculations were performed for a square lattice, which corresponds to the quasi-two-dimensional structure of CeRhIn₅ [3]. The Hamiltonian $\hat{\mathcal{H}}_{c0}$ describes the system of itinerant c electrons. Operators $c_{m\sigma}$ ($c_{m\sigma}^\dagger$) are Fermi creation (annihilation) operators of a c electron at the site m with the spin projection σ . The parameter ε_0 defines the electron energy at the site and μ is the chemical potential of the system. The intensity of hopping of c electrons between the sites l and m is given by the matrix elements t_{ml} .

The term $\hat{\mathcal{H}}_{f0}$ is responsible for the existence of the states of f electrons forming the localized energy level with the bare energy E_0 . By definition, the Hubbard operators $X_m^{r_l} = |mr\rangle\langle tl|$ perform the transition from the state $|mt\rangle$ to the state $|mr\rangle$ at the site m .

The coupling between the two subsystems of electrons is fixed by the Hamiltonian $\hat{\mathcal{H}}_{\text{mix}}$ describing the intra-atomic ($m = l$) and interatomic ($m \neq l$) hybridization mixing of c and f states with the amplitude V_{ml} .

In the operator of the superexchange interaction $\hat{\mathcal{H}}_{\text{exch}}$, \mathbf{S}_m is the quasi-spin vector operator and \hat{N}_m is the operator of the number of f electrons.

3. To study the coexistence phase of antiferromagnetism and superconductivity in the heavy-fermion systems, we use the equations of motion with the projection technique, which is often applied in the theory of superconductivity of strongly correlated systems

[13, 14]. The exact equations of motion for the operators are represented in the form

$$\begin{aligned} i \frac{dX_f^{0\sigma}}{dt} &= (E_0 - \mu) X_f^{0\sigma} \\ &+ \sum_f V_{ff}^* [(X_f^{00} + X_f^{\sigma\sigma}) a_{f\sigma} + X_f^{\bar{\sigma}\sigma} a_{f'\bar{\sigma}}] \\ &+ \sum_g W_{gf}^* [(X_f^{00} + X_f^{\sigma\sigma}) b_{g\sigma} + X_f^{\bar{\sigma}\sigma} b_{g\bar{\sigma}}] \\ &+ \sum_{\langle g \rangle} \left(\frac{J_{fg}}{2} \right) (X_f^{0\bar{\sigma}} Y_g^{\bar{\sigma}\sigma} - X_f^{0\sigma} Y_g^{\bar{\sigma}\bar{\sigma}}), \\ i \frac{dY_g^{0\sigma}}{dt} &= (E_0 - \mu) Y_g^{0\sigma} \\ &+ \sum_{g'} V_{g'g}^* [(Y_g^{00} + Y_g^{\sigma\sigma}) b_{g'\sigma} + Y_g^{\bar{\sigma}\sigma} b_{g'\bar{\sigma}}] \\ &+ \sum_f W_{fg}^* [(Y_g^{00} + Y_g^{\sigma\sigma}) a_{f\sigma} + Y_g^{\bar{\sigma}\sigma} a_{f\bar{\sigma}}] \\ &+ \sum_{\langle f \rangle} \left(\frac{J_{fg}}{2} \right) (X_f^{\bar{\sigma}\sigma} Y_g^{0\bar{\sigma}} - X_f^{\bar{\sigma}\bar{\sigma}} Y_g^{0\sigma}), \\ i \frac{da_{f\sigma}}{dt} &= (\varepsilon_0 - \mu) a_{f\sigma} + \sum_f (t_{ff'} a_{f'\sigma} + V_{ff'} X_f^{0\sigma}) \\ &+ \sum_g (t_{fg} b_{g\sigma} + W_{fg} Y_g^{0\sigma}), \\ i \frac{db_{g\sigma}}{dt} &= (\varepsilon_0 - \mu) b_{g\sigma} + \sum_{g'} (t_{gg'} b_{g'\sigma} + V_{gg'} Y_{g'}^{0\sigma}) \\ &+ \sum_f (t_{gf} a_{f\sigma} + W_{gf} X_f^{0\sigma}). \end{aligned}$$

In these equations, the division into two antiferromagnetic sublattices was performed. The operators $X_{f(f', f'', \dots)}^{r_l}$ and $a_{f(f', f'', \dots)\sigma}$ act on the states of the f and c electrons, respectively, at sites $f(f', f'', \dots)$ belonging to the F sublattice for which $\langle S_f^z \rangle \geq 0$. Operators $Y_{g(g', g'', \dots)}^{r_l}$ and $b_{g(g', g'', \dots)\sigma}$ refer to the G sublattice and $\langle S_g^z \rangle = -\langle S_f^z \rangle$. Indices in angular brackets in the above equations of motion mean that the superexchange interaction occurs only between the nearest f electrons being in different sublattices. In the two-sublattice description, the parameter W_{fg} denotes the hybridization integral between c and f electrons from different sublattices. The previous notation ($V_{ff'}$, $V_{gg'}$) is kept for the intensity of the hybridization processes inside one sublattice.

Further in the written equations of motion, we perform the projection of their right-hand parts on the basis of operators constituting an orthogonal set:

$$\mathbf{e} = (X_f^{0\sigma}, Y_g^{0\sigma}, a_{f\sigma}, b_{g\sigma}, X_f^{\bar{0}}, Y_g^{\bar{0}}, a_{f\bar{\sigma}}, b_{g\bar{\sigma}}). \quad (2)$$

The procedure of the operator projection is performed according to the algorithm described in [15]. The normalization factors of the Hubbard basis operators are defined in the form

$$\alpha_\sigma = \alpha + \eta_\sigma R, \quad \alpha = 1 - n_L/2. \quad (3)$$

Here, the magnetization value of the F sublattice is denoted as $R = \langle S_f^z \rangle$ and the average on-site number of localized f electrons is $n_L = \langle N_f \rangle$. The σ -dependent function η_σ is conventionally defined: $\eta_\sigma = 1$ if $\sigma = \uparrow$ and $\eta_\sigma = -1$ if $\sigma = \downarrow$.

To describe anomalous pairing leading to superconductivity, we derive Hermitian-conjugate equations of motion at $\sigma \rightarrow \bar{\sigma}$. Further, we take into account only the mean-field corrections and averages determining the anomalous pairing of the nearest f electrons in different sublattices. Then, a system of equations for the Fourier transforms of the irreducible Green's functions in the quasi-momentum space has the form

$$\begin{bmatrix} \hat{F}_{p\sigma}(\omega) & \hat{G}_{p\sigma} \\ -\hat{G}_{-p\bar{\sigma}}^* & -\hat{F}_{-p\bar{\sigma}}^*(-\omega) \end{bmatrix} \langle\langle \mathbf{e}_p | B \rangle\rangle_\omega = \langle \{ \mathbf{e}_p, B \}_+ \rangle. \quad (4)$$

Here, \mathbf{e}_p consists of the Fourier transforms of the basis operators. To write Eq. (4), the definitions for the fourth-order matrices were introduced:

$$\hat{F}_{p\sigma}(\omega) = \begin{bmatrix} \omega - E_\sigma & 0 & -\alpha_\sigma V_p^* & -\alpha_\sigma W_p^* \\ 0 & \omega - E_{\bar{\sigma}} & -\alpha_{\bar{\sigma}} W_p^* & -\alpha_{\bar{\sigma}} V_p^* \\ -V_p & -W_p & \omega - \xi_p & -\Gamma_p \\ -W_p & -V_p & -\Gamma_p & \omega - \xi_p \end{bmatrix}, \quad (5)$$

$$\hat{G}_{p\sigma} = - \begin{bmatrix} 0 & \eta_\sigma \Delta_p / \alpha_\sigma & 0 & 0 \\ \eta_\sigma \Delta_{-p} / \alpha_{\bar{\sigma}} & 0 & 0 & 0 \\ 0 & 0 & 0 & 0 \\ 0 & 0 & 0 & 0 \end{bmatrix}, \quad (6)$$

where $E_\sigma = E_0 - \mu - (J_0/2)(n_L/2 + \eta_\sigma R)$ and $\xi_p = \varepsilon_0 - t_p - \mu$. The functions t_p , Γ_p , V_p , and W_p are determined in terms of the Fourier transforms of the intrasublattice and intersublattice hopping and hybridization parameters (t_{ff} , t_{fg} , V_{ff} , and W_{fg} , respectively). The

superconducting order parameter Δ_p gives the intensity of the Cooper pairing:

$$\Delta_p = \frac{1}{N/2} \sum_q \frac{1}{2} [J_{p-q} \langle X_{q\uparrow} Y_{-q\downarrow} \rangle + J_{p+q} \langle Y_{q\uparrow} X_{-q\downarrow} \rangle]. \quad (7)$$

From system (4), we find the Fourier transforms of the basis Green's functions required for the further investigations:

$$\langle\langle X_{p\sigma} | X_{p\sigma}^\dagger \rangle\rangle_\omega = \langle\langle Y_{p\bar{\sigma}} | Y_{p\bar{\sigma}}^\dagger \rangle\rangle_\omega = \frac{\alpha_\sigma M_{p\sigma}^{11}(\omega)}{D_{8\sigma}(p, \omega)}, \quad (8)$$

$$\langle\langle a_{p\sigma} | a_{p\sigma}^\dagger \rangle\rangle_\omega = \langle\langle b_{p\bar{\sigma}} | b_{p\bar{\sigma}}^\dagger \rangle\rangle_\omega = \frac{M_{p\sigma}^{33}(\omega)}{D_{8\sigma}(p, \omega)}, \quad (9)$$

where $D_{8\sigma}(p, \omega)$ is the determinant of the matrix of the system of equations (4) and $M_{p\sigma}^{ij}(\omega)$ is the determinant of the matrix deduced from matrix (4) by deleting the i th row and j th column. The explicit expressions for these functions are not given because they are very lengthy.

The Fourier transform of the anomalous Green's function has the form

$$\langle\langle Y_{-p\bar{\sigma}} | X_{p\sigma} \rangle\rangle_\omega = -\frac{\alpha_\sigma M_{-p\bar{\sigma}}^{52}(\omega)}{D_{8\sigma}(p, \omega)}. \quad (10)$$

To calculate the determinant $M_{-p\bar{\sigma}}^{52}(\omega)$, in addition to deleting the corresponding rows and columns in matrix (4), it is necessary to make the replacements $p \rightarrow -p$, $\sigma \rightarrow \bar{\sigma}$.

The energy structure is determined from the condition $D_{8\sigma}(p, \omega) = 0$. The positive definite solutions of this equation correspond to the four branches of the spectrum of collective excitations.

The unknown quantities of the model are μ , n_L , R , and Δ_p . We use the spectral theorem in order to determine them. After some simplifications, we find an equation relating the Green's function given by Eqs. (8)–(10) to the thermodynamic averages:

$$\langle \hat{A}_f \hat{B}_f \rangle = \frac{1}{N/2} \sum_{k\lambda} \frac{e^{ik(f-f')}}{2E_{\lambda k} \prod_{\nu \neq \lambda} (E_{\lambda k}^2 - E_{\nu k}^2)} \times [L_k(E_{\lambda k})f(E_{\lambda k}) - L_k(-E_{\lambda k})f(-E_{\lambda k})], \quad (11)$$

where $f(x) = 1/(e^{x/T} + 1)$ is the Fermi–Dirac distribution function, T is temperature, $E_{\lambda k}$ ($\lambda = 1, \dots, 4$) are the positive definite branches of the energy spectrum, and $L_k(\omega)$ is the numerator of the Green's

function $\langle\langle B_k|A_k \rangle\rangle_\omega$. Then, the Green's function given by Eq. (8) is used to calculate the parameters

$$n_L = \sum_{\sigma} \langle X_f^{\sigma\sigma} \rangle, \quad R = (\langle X_f^{\uparrow\uparrow} \rangle - \langle X_f^{\downarrow\downarrow} \rangle) / 2. \quad (12)$$

The concentration of c electrons is given by the expression

$$n_c = \sum_{\sigma} \langle a_{f\sigma}^{\dagger} a_{f\sigma} \rangle, \quad (13)$$

where the average is expressed in terms of Eq. (9). It is easy to show that the self-consistency equation on μ for the chosen value of the total concentration of electrons n_e in the system has the form

$$n_e = n_L + n_c = \sum_{\sigma} (\langle X_f^{\sigma\sigma} \rangle + \langle a_{f\sigma}^{\dagger} a_{f\sigma} \rangle). \quad (14)$$

The substitution of the expression relating $\langle X_{q\sigma} Y_{-q\bar{\sigma}} \rangle$ to the Fourier transform of the Green's function given by Eq. (10) into definition (7) of the superconducting order parameter leads to the integral self-consistency equation. It has several solutions corresponding to the different types of quasi-momentum dependence Δ_p . The character of the kernel of the integral equations which is split due to the presence of $J_{p\pm q}$ makes it possible to find the explicit form of Δ_p accurate within an unknown amplitude. The amplitude Δ_0 is determined from the algebraic equation the form of which depends on the symmetry of Δ_p :

$$\Delta_0 = J \frac{1}{N/2} \sum_{q\lambda} Z_q [\alpha_{\uparrow} M_{-q\downarrow}^{52}(E_{\lambda,q}) - \alpha_{\downarrow} M_{q\uparrow}^{52}(E_{\lambda,q})] \times \frac{\tanh(E_{\lambda,q}/2T)}{2E_{\lambda,q} \prod_{v \neq \lambda} (E_{\lambda,q}^2 - E_{vq}^2)}. \quad (15)$$

Here,

$$Z_q = \cos(q_x b/2) \cos(q_y b/2) \quad (16)$$

or

$$Z_q = \sin(q_x b/2) \sin(q_y b/2), \quad (17)$$

if Δ_p has s or d symmetry in the magnetic Brillouin zone, respectively,

$$\Delta_p = 2\Delta_0^s \cos(p_x b/2) \cos(p_y b/2), \quad (18)$$

$$\Delta_p = 2\Delta_0^d \sin(p_x b/2) \sin(p_y b/2). \quad (19)$$

In Eq. (15), it was taken into account that $M_{-p\bar{\sigma}}^{52}(\omega)$ is an even function of ω and contains contributions proportional only to Δ_p and Δ_p^3 .

At present, there is no commonly accepted opinion concerning the symmetry of the superconducting order parameter in the coexistence phase of antiferromagnetism and superconductivity of CeRhIn₅. Nuclear quadrupole resonance experiments in the superconducting phase of CeRhIn₅ when the long-range antiferromagnetic order is completely suppressed by the applied pressure determine the cubic temperature dependence of the spin–lattice relaxation rate [16]. It is considered that this dependence corresponds to the formation of d -wave superconductivity with nodes on the Fermi surface, at which the superconducting gap becomes zero. However, as was experimentally shown at lower pressures, this dependence in the coexistence phase of antiferromagnetism and superconductivity is modified into a linear dependence on the temperature [17]. The linear dependence may result from the formation of gapless p -wave superconductivity [18] or d -wave superconductivity with the additional nodes on the Fermi surface [19]. The measurements of the specific heat under the magnetic field rotation in the coexistence phase of antiferromagnetism and superconductivity also indicate the implementation of the preferably d -wave superconducting order parameter but with additional nodes [20]. In view of this circumstance, in contrast to [9], where only the s -wave superconducting order parameter was considered, we study the case where the Cooper instability leads to the appearance of the experimentally observed d -wave superconductivity.

It is important that, to implement the long-range antiferromagnetic order, the chemical potential should lie in the weakly dispersive heavy-fermion band. Since the explicit form of the spectrum of elementary excitations corresponding to the formation of heavy fermions is lengthy, we present the approximate expression

$$E_{2p} \approx \sqrt{[E_p^{afm}]^2 + \zeta_p \Delta_p^2}, \quad (20)$$

$$\zeta_p = \frac{\alpha^2 + R^2}{(\alpha^2 - R^2)^2} - \frac{R^2}{(\alpha^2 - R^2)[(1 - \alpha\gamma_p)E_J - \mu] \lambda_p} \times \left\{ \Gamma_p^2 \gamma_p^2 + \frac{2\alpha}{\alpha^2 - R^2} [(1 - \alpha\gamma_p)E_J - \mu](\gamma_p E_J + J_0/2) \right\},$$

$$E_p^{afm} = |(1 - \alpha\gamma_p)E_J - \mu| - \lambda_p, \quad (21)$$

$$E_J = E_0 - \frac{J_0 N_L}{4} \quad (J_0 = 4J), \quad \gamma_p = \frac{V_p^2}{\Gamma_p^2 - E_J^2},$$

$$\lambda_p = \sqrt{(\alpha^2 - R^2) \Gamma_p^2 \gamma_p^2 + (\gamma_p E_J + J_0/2)^2 R^2}.$$

It is easy to show that the width of the gap in the spectrum of elementary excitations is determined by the parameter $\Psi_p = \sqrt{\zeta_p} \Delta_p$.

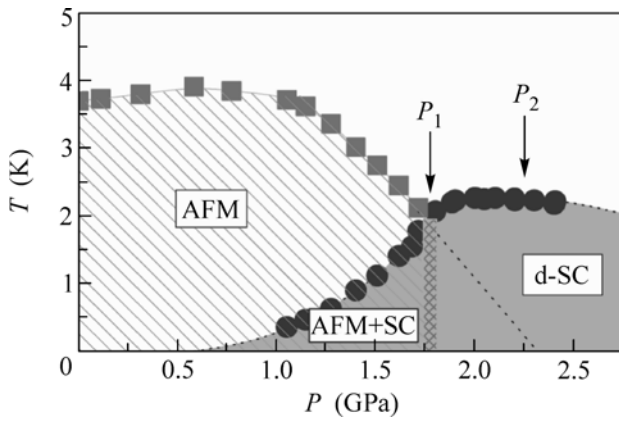


Fig. 1. Phase diagram of CeRhIn₅ [22].

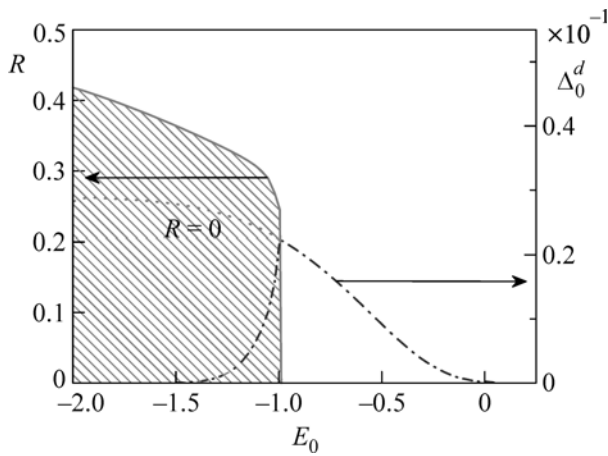


Fig. 2. Variation of the magnetization of the antiferromagnetic sublattice R and amplitude of the d -wave superconducting order parameter Δ_0^d with increasing energy E_0 .

The effective mass of heavy fermions whose energies E_{2p} are given by Eq. (20) is estimated from the expression

$$\frac{m^*}{m_0} = \frac{\Gamma_0^2 - E_J^2}{|\Gamma_0| \gamma_0} \left\{ 2\alpha |E_J| - \frac{1}{\lambda_0} [(\alpha^2 - R^2)\Gamma_0^2 \gamma_0 + (\alpha^2 + R^2)E_J^2 \gamma_0 - J_0 R^2 |E_J|] \right\}^{-1}, \quad (22)$$

where $m_0 = \hbar^2 / (|t_1| b^2)$ is the mass of the Bloch electron on a square lattice near the band bottom. The quantities Γ_0 , γ_0 , and λ_0 are obtained from known Γ_p , γ_p , and λ_p at $p_x = p_y = 0$. A similar method in the slave-boson representation was used in [21] to estimate the mass of heavy fermions of antiferromagnetic intermetallics taking into account the canting of the antiferromagnetic sublattices.

4. The study of the temperature dependence of the specific heat of the heavy-fermion compound CeRhIn₅ at different values of the external pressure [22] allowed the establishment of the shape of the temperature–pressure phase diagram of this intermetallic (Fig. 1). Squares in the figure correspond to the temperatures of the transition (T_N) from the paramagnetic state to the antiferromagnetic phase. Points denote critical temperatures (T_c) of the transition from the normal phase to the superconducting phase. It can be seen that, if the further decrease in the temperature in the antiferromagnetic phase induces the Cooper instability, then the system transfers to the coexistence phase of antiferromagnetism and superconductivity. The notation P_1 corresponds to the pressure at which the long-range antiferromagnetic order is completely destroyed.

The shape of the phase diagram indicates competition between the antiferromagnetic ordering and superconductivity in CeRhIn₅. Indeed, the considerable suppression of T_N starts when superconductivity is formed. At the critical point P_1 when the antiferromagnetic phase is destroyed, the superconducting phase has T_c close to the maximum. It should be noted that, in spite of the obvious competition between the superconducting and antiferromagnetic orders, no phase separation occurs. According to the nuclear quadrupole resonance [23] and neutron diffraction [24] data, both ordering types coexist on the microscopic level in the coexistence phase of antiferromagnetism and superconductivity.

Figure 2 shows the calculated dependences of the magnetization of the antiferromagnetic sublattice R and the amplitude of the d -wave superconducting order parameter on the energy of the localized level E_0 at the constant concentration $n_e = 1.25$. We chose the parameters $J = 0.2$ and $V_0 = 0.6$ (in units of the amplitude of hopping $|t_1|$ of c electrons between nearest neighbors). The values of the concentration of the f electrons n_L and the chemical potential μ were found in a self-consistent manner. The effect of pressure on the electron structure of the studied heavy-fermion intermetallic was simulated by changing the position of the bare energy level of the localized electrons. This approach was successfully applied when studying the systems with the intermediate valence of the f states [25]. In CeRhIn₅, the energy E_0 shifts with increasing pressure due to an increase in the Coulomb interaction of the $4f$ electron Ce³⁺ with the effectively negative charge on the nearest ions. Therefore, the increase in E_0 corresponds to the application of increasing pressure. In [7, 8], the pressure effect on the system was reduced to the change in the hopping, hybridization, and exchange parameters, as well as in the density of states $\rho(E_F)$.

It is seen that, at the chosen model parameters, an increase in the pressure leads to the destruction of the

long-range antiferromagnetic ordering (solid lines). The superconducting phase is implemented at high pressures. The dependence of Δ_0^d on E_0 is shown by a dash-dotted line. The behavior of the superconducting order parameter changes sharply in the region of the implementation of the antiferromagnetic state. If the long-range antiferromagnetic order were not established, then the dependence of Δ_0^d on E_0 would be represented by the dotted line. However, the appearance of the antiferromagnetic order parameter qualitatively changes this dependence, leading to the sharp decrease in Δ_0^d (see the dash-dotted line in the region of the implementation of the antiferromagnetic phase). On the one hand, this demonstrates the competition between the superconductivity and antiferromagnetism. On the other hand, it clearly shows the presence of the region of the coexistence phase of antiferromagnetism and superconductivity. With an increase in the antiferromagnetic order parameter in this region, Δ_0^d quickly vanishes. In this respect, we emphasize that the suppressing effect of the long-range antiferromagnetic order on the Cooper pairing is due not only to the decrease in the amplitude Δ_0^d but also to the reduction of the superconducting gap at $R \neq 0$ in the spectrum of the elementary excitations (see Eq. (20)).

We consider the experimental observations of an increase in the Sommerfeld constant [26] as well as the cyclotron [27] and effective [28] electron mass in CeRhIn₅ with increasing pressure. The increase in the effective fermion mass in our approach is observed near the region of coexistence of antiferromagnetism and superconductivity (Fig. 3). The effective mass is calculated according to Eq. (22) on the basis of self-consistent solutions. It is seen that the effective mass of heavy fermions at atmospheric pressure (it corresponds to the energy $E_0 \approx -2$) exceeds the mass of free fermions by a factor of about 25. With increasing pressure, the effective mass increases considerably. The maximum sharp increase in the mass is achieved when approaching the critical point, at which the antiferromagnetic order is completely destroyed ($R = 0$). The change in the sign of the effective mass of heavy fermions at the critical pressure occurs due to the change of the carrier type at the transfer from the antiferromagnetic to the paramagnetic phase [29]. The absolute value of the quantity m^*/m_0 decreases when the pressure increases further.

5. In conclusion, we summarize the results obtained due to using the microscopic approach. The inclusion of the antiferromagnetic coupling between the localized electrons of the rare-earth subsystem made it possible both to describe the antiferromagnetic and d -wave superconducting phases and to obtain the conditions of the implementation of the state in which

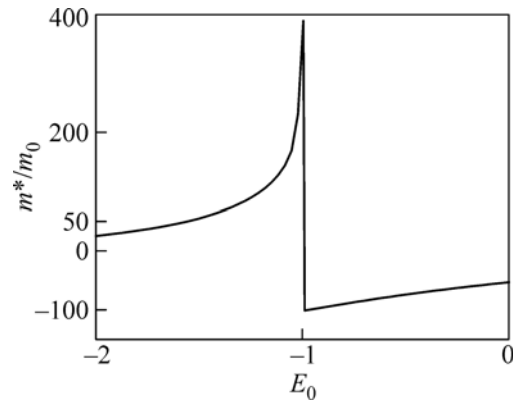


Fig. 3. Effective fermion mass normalized to the free electron mass versus E_0 .

antiferromagnetism and superconductivity coexist at the microscopic level. It is important that the microscopic description of the superconducting phase in the presence of long-range antiferromagnetic order requires the inclusion of two types of anomalous averages due to the existence of two magnetic sublattices. These anomalous averages are characterized by different temperature dependences closely related to a particular symmetry of the superconducting order parameter. Our conclusions about the coexistence phase of antiferromagnetism and superconductivity are in good qualitative agreement with the experimental data on the implementation of this phase in heavy-fermion intermetallic CeRhIn₅.

The microscopic mechanism of the increase in the effective fermion mass has been revealed in this work. Conclusions made on its basis are in qualitative agreement with the experimental data indicating the considerable increase in the effective fermion mass with increasing pressure near the point of the destruction of antiferromagnetism.

This work was supported by the Presidium of the Russian Academy of Sciences (program “Quantum Mesoscopic and Disordered Structures”), the Russian Foundation for Basic Research (project nos. 10-02-00251 and 11-02-98007-Siberia), and the Ministry of Education and Science of the Russian Federation (federal program “Human Capital for Science and Education in Innovative Russia” for 2009–2013).

REFERENCES

1. C. Pfleiderer, *Rev. Mod. Phys.* **81**, 1551 (2009).
2. N. D. Mathur, F. M. Grosche, S. R. Julian, et al., *Nature* **394**, 39 (1998).
3. H. Hegger, C. Petrovic, E. G. Moshopoulou, et al., *Phys. Rev. Lett.* **84**, 4986 (2000).
4. M. Nicklas, V. A. Sidorov, H. A. Borges, et al., *Phys. Rev. B* **67**, 020506 (2003).
5. S. Nakatsuji, D. Pines, and Z. Fisk, *Phys. Rev. Lett.* **92**, 016401 (2004).

6. Yi-feng Yang, Z. Fisk, Han-Oh Lee, et al., *Nature* **454**, 611 (2008).
7. Yi-feng Yang, N. J. Curro, Z. Fisk, et al., *J. Phys.: Conf. Ser.* **273**, 012066 (2011).
8. P. D. Sacramento, *J. Phys.: Cond. Mat.* **15**, 6285 (2003).
9. J. V. Alvarez and F. Yundurain, *Phys. Rev. Lett.* **98**, 126406 (2007).
10. T. Park and J. D. Thompson, *New J. Phys.* **11**, 055062 (2009).
11. V. Barzykin, *Phys. Rev. B* **73**, 094455 (2006).
12. V. V. Val'kov and D. M. Dzebisashvili, *Theor. Math. Phys.* **157**, 1565 (2008).
13. N. M. Plakida, *Theor. Math. Phys.* **154**, 108 (2008).
14. N. M. Plakida, *High-Temperature Cuprate Superconductors. Experiment, Theory, and Applications* (Springer, Berlin, 2008).
15. H. Mori, *Prog. Theor. Phys.* **33**, 423 (1965).
16. Y. Kohori, Y. Yamato, Y. Iwamoto, and T. Kohara, *Eur. Phys. J. B* **18**, 601 (2000).
17. S. Kawasaki, T. Mito, Y. Kawasaki, et al., *Phys. Rev. Lett.* **91**, 137001 (2003).
18. Y. Fuseya, H. Kohno, and K. Miyake, *J. Phys. Soc. Jpn.* **72**, 2914 (2003).
19. Y. Bang, M. J. Graf, A. V. Balatsky, and J. D. Thompson, *Phys. Rev. B* **69**, 014505 (2004).
20. T. Park, E. D. Bauer, and J. D. Thompson, *Phys. Rev. Lett.* **101**, 177002 (2008).
21. V. V. Val'kov and D. M. Dzebisashvili, *J. Exp. Theor. Phys.* **110**, 301 (2010).
22. T. Park, Y. Tokiwa, E. D. Bauer, et al., *Physica B* **403**, 943 (2008).
23. T. Mito, S. Kawasaki, Y. Kawasaki, et al., *Phys. Rev. Lett.* **90**, 077004 (2003).
24. A. Llobet, J. S. Gardner, E. G. Moshopoulou, et al., *Phys. Rev. B* **69**, 024403 (2004).
25. D. I. Khomskii, *Sov. Phys. Usp.* **22**, 879 (1979).
26. R. A. Fisher, F. Bouquet, N. E. Phillips, et al., *Phys. Rev. B* **65**, 224509 (2002).
27. H. Shishido, R. Settai, H. Harima, and Y. Ōnuki, *J. Phys. Soc. Jpn.* **74**, 1103 (2005).
28. G. Knebel, D. Aoki, J.-P. Brison, and J. Flouquet, *J. Phys. Soc. Jpn.* **77**, 114704 (2008).
29. V. V. Val'kov and D. M. Dzebisashvili, *Theor. Math. Phys.* **162**, 106 (2010).

Translated by L. Mosina